Polymer Degradation and Stability 102 (2014) 180–185

Contents lists available at ScienceDirect

Polymer Degradation and Stability

journal homepage: www.elsevier.com/locate/polydegstab

The effect of zirconium incorporation on the thermal stability and carbonized product of phenol–formaldehyde resin

Changqing Liu, Kezhi Li*, Hejun Li, Shouyang Zhang, Yulei Zhang

State Key Laboratory of Solidification Processing, Carbon/Carbon Composites Research Center, Northwestern Polytechnical University, Xi'an 710072, PR China

ARTICLE INFO

Article history:
Received 11 August 2013
Received in revised form
12 December 2013
Accepted 12 January 2014
Available online 22 January 2014

Keywords:
Phenolic resin
Zirconium
Modified
Thermal stability
Carbonization

ABSTRACT

A kind of zirconium modified phenolic resin (Zr-PF) was prepared by using phenol, paraformaldehyde, $ZrOCl_2 \cdot 8H_2O$, acetylacetone, ethanol and H_2O_2 as raw materials. The structure of the Zr-PF was characterized by Fourier transform infrared (FT-IR) spectra and solution ^{13}C nuclear magnetic resonance (^{13}C NMR) spectra. The viscosity and thermal degradation behaviors of the Zr-PF were studied by rotary viscometer and thermogravimetric analyzer–differential scanning calorimetry (TG-DSC), respectively. The carbonized products of ordinary phenolic resin (PF) and Zr-PF were further investigated by X-ray diffraction (XRD), laser Raman spectroscopy (Raman) and scanning electron microscopy (SEM). Results show that new chemical bonds are formed through coordination reactions between zirconium atoms in Zr–OH and oxygen atoms in the acetylacetone and hydroxymethyl phenols. Viscosity of the Zr-PF is higher than that of PF during 30–80 °C. Compared with PF, thermal stability of the Zr-PF is obviously improved and its char yield is 55% at 1200 °C, 8% higher than that of PF. The d_{002} value of carbonized Zr-PF decreases from 0.3470 nm (carbonized PF) to 0.3329 nm and its crystallite height increases from 23.89 nm (carbonized PF) to 29.21 nm due to zirconium incorporation. In addition, the ID/(ID + IG) value of carbonized Zr-PF decreases from 0.571 (carbonized PF) to 0.364 and the crystallite size of it increases from 29.90 nm (carbonized PF) to 44.79 nm. The results prove that the incorporation of zirconium exhibits obvious effects on promoting its graphite crystallite. What is more, the morphology of the carbonized Zr-PF changes from poor structure with many pore defects into dense and uniform matrix with uniformly dispersed ZrC particles.

1. Introduction

Phenol–formaldehyde resin (PF) is still used as a precursor for the matrix of carbon/carbon composites due to its good mechanical properties and heat resistance after carbonization. In recent years, much efforts has been made to improve its mechanical properties and heat resistance by incorporating functional groups or other elements into polymer chain of phenolic resin such as boron, silicon, titanium and phosphorus etc. [1–5]. These modified resins are widely used in the process of polymer infiltration and pyrolysis technique to prepare refractory carbide modified carbon/carbon composites (C/C) in order to improve the ablation resistance of C/C by forming ceramic particles [6–8]. Zirconium tends to form Zr–O bond with a bond energy of 776 kJ mol^{-1}, which is much higher than that of C–C bond of 345 kJ mol^{-1} [9]. Therefore, the thermal stability of phenolic resin would be improved after modified by zirconium and it may also be an effective way to use it as an organic precursor to prepare zirconium modified carbon/carbon composites. Furthermore, it is found that zirconium can also improve the graphitization of disordered carbon materials [10]. Wang [11] tried to prepare zirconium modified phenolic resin (Zr-PF) by using phenol, paraformaldehyde, $ZrOCl_2 \cdot 8H_2O$ as raw materials, but the difficulties in controlling the reaction process and viscosity of the obtained product limited the further development of Zr-PF. While there are few reports about zirconium modified phenolic resin so far. Moreover, the effect of zirconium element on the properties of PF, especially on the pyrolysis and carbonization has not been further studied.

In the present work, phenol, paraformaldehyde, $ZrOCl_2 \cdot 8H_2O$, acetylacetone, ethanol and H_2O_2 were used as raw materials to introduce zirconium into phenolic resin through chemical reactions. The reaction process was easily controlled to avoid gelation and the product was kept in low viscosity. Structure of the Zr-PF was characterized by Fourier transform infrared (FT-IR) spectra and solution ^{13}C nuclear magnetic resonance (^{13}C–NMR) spectra. Viscosity and thermal degradation behavior of the resin were

* Corresponding author. Tel./fax: +86 29 88495764.
E-mail address: likezhi@nwpu.edu.cn (K. Li).

0141-3910/$ – see front matter © 2014 Elsevier Ltd. All rights reserved.
http://dx.doi.org/10.1016/j.polymdegradstab.2014.01.013

analyzed by rotary viscometer and thermogravimetric analyzer–differential scanning calorimetry (TG–DSC). In addition, carbonized products of the Zr-PF and PF were also analyzed by X-ray diffraction (XRD), laser Raman spectroscopy (Raman) and scanning electron microscopy (SEM), respectively.

2. Experimental

2.1. Materials

Phenol and paraformaldehyde (PA) were obtained from Tianjin Fuchen Chemical Reagent Co., Ltd.; zirconium oxychloride ($ZrOCl_2 \cdot 8H_2O$), ethanol, acetylacetone were obtained from Tianjin Fengyue Chemical Reagent Co., Ltd.; H_2O_2 (concentration: 30%) and NaOH were obtained from Tianjin Fuyu Chemical Reagent Company. All reagents were used as received.

2.2. Synthesis of zirconium modified phenolic resin

The zirconium modified phenolic resin (Zr-PF) was synthesized as presented in Fig. 1. Phenol, paraformaldehyde and NaOH were added into a three-necked flask placed in a heated water bath equipped with a condenser and a mechanical stirrer. The mixture was stirred to be a homogeneous solution, and reacted at 70–75 °C for 1–1.5 h. Then an inorganic hybrid solution which was prepared by dissolving $ZrOCl_2 \cdot 8H_2O$, Hacac and H_2O_2 in ethanol was added into the solution and reacted at 90 °C for 1–2 h. A red–brown semi-liquid product Zr-PF was obtained by removing residual solvent. And the phenolic resin with zirconium content from 0 to 20% would be synthesized by changing $ZrOCl_2 \cdot 8H_2O$ inorganic hybrid solution molarity. In the following research, phenolic resin with zirconium content of 10% was mainly studied as representative sample. The ordinary PF was also prepared with the same process for comparison.

2.3. Purification of zirconium modified phenolic resin

To eliminate the effect of residual reactants, especially the $ZrOCl_2 \cdot 8H_2O$ inorganic hybrid solution, on the test results of obtained zirconium modified phenolic resin (Zr-PF), Zr-PF was purified by the following steps. Firstly, the Zr-PF was added into dilute sodium hydroxide solution, and then washed the resulting precipitate with deionized water for 3–4 times. Finally, the precipitate was removed by sedimentation in the centrifuge using deionized water as a solvent. After having repeated these steps for three times, the final product was dried in vacuum oven for 3 h at 65 °C. Thus the purified Zr-PF without curing was used as the sample in the following characterization and heat-treatment.

2.4. Characterization

The structure of the Zr-PF was characterized (coating method) by FT-IR (Vector-22, Bruker, Germany) and solution ^{13}C–NMR (Mercury Plus Varian-300, Varian, USA) using DMSO as a solvent. Viscosity of the resin was analyzed by rotary viscometer (NDJ-5S, Changji, China). Thermal degradation behavior of the resin was analyzed by means of TG-DSC (STA429CD/3/7, Netzsch, Germany) at a heating rate of 5 °C min^{-1} from 30 °C to 1200 °C in nitrogen atmosphere. To further investigate the effect of zirconium on microstructure of carbonized PF, carbonized products of the PF and Zr-PF were studied by Raman (Renishaw, United Kingdom) and XRD (X'Pert Pro MPD, PANalytical, Netherlands). The heat treatment of both samples was carried out in a graphite crucible using a high-temperature graphite resistance furnace (ZGSS-400, Jinzhou, China) at temperature of 2000 °C for 2 h in argon gas with a heating rate of 10 °C min^{-1}, then cooled to room temperature slowly. Morphology of the carbonized products was analyzed by SEM (Amray 1000B, USA).

3. Results and discussion

3.1. Chemical structure of zirconium modified phenolic resin (Zr-PF)

A comparison of FT-IR spectra of PF and Zr-PF is shown in Fig. 2. The characteristic absorption peaks of the Zr-PF are shown in Table 1. The peaks at 1597 cm^{-1} and 1506 cm^{-1} are due to C=C stretching of benzene rings and peaks at 888 cm^{-1}, 821 cm^{-1}, 757 cm^{-1} could be assigned to C–H flexural vibration of benzene rings. All of these bands are characteristic absorption bands of PF. While compared with the curve of PF, an increase in the band at 1450 cm^{-1} (stretching vibration of C=O) indicates that coordination compound was obtained by coordination reaction between $ZrOCl_2 \cdot 8H_2O$ hydrolyzates (Zr–OH) and acetylacetone [12]. Moreover, the band at 560 cm^{-1} is assigned to be the vibration of Zr–O [13]. As the effect of residual reactants (especially the $ZrOCl_2 \cdot 8H_2O$ inorganic hybrid solution) has been eliminated, the appearance of Zr–O absorption peak is believed to be caused by the zirconium introduced into the reaction product. Based on the analysis above, it can be concluded that zirconium has been incorporated into the reaction product and exists in the form of Zr–O bond.

A comparison of ^{13}C NMR spectra of PF and Zr-PF is shown in Fig. 3. The major chemical shifts the PF and Zr-PF are summarized in Table 2. Compared with the ^{13}C NMR spectra of PF, chemical

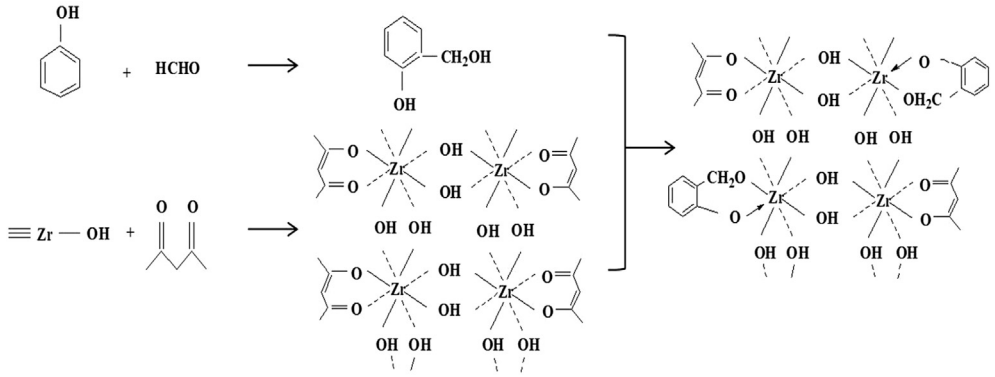

Fig. 1. Reaction scheme for preparation of the zirconium modified phenolic resin.

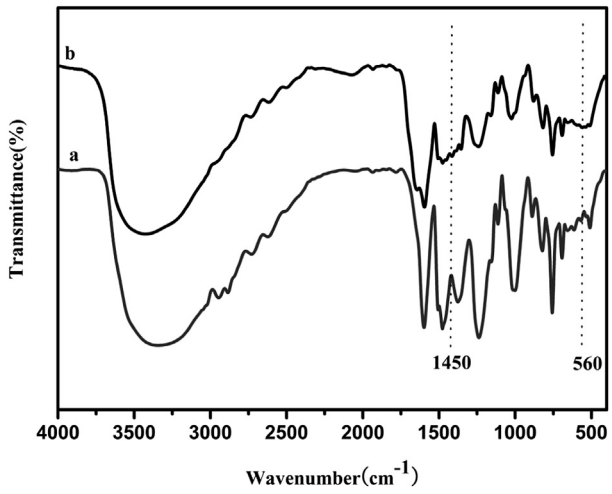

Fig. 2. FT-IR spectra of ordinary phenolic resin and zirconium modified phenolic resin, a) ordinary phenolic resin, b) zirconium modified phenolic resin.

structure modifications of the Zr-PF can be deduced [14]. From ^{13}C NMR spectra of Zr-PF, no shifts at 35–50 ppm which are attributed to methylene bridge carbons are observed [15]. This indicates that the further reaction between hydroxymethyl phenols may not occur. In addition, it can be observed that chemical shifts of carbons in phenol ring of Zr-PF shift to lower field compared with the carbons in phenol ring of PF, which indicates that hydroxymethyl phenols in Zr-PF should be bonded with a strong electrophilic group and this group could be explained by the zirconium-containing coordination compound formed between Zr–OH and acetylacetone. Moreover, it is found that the chemical shifts of the carbons (–CH_3 in acetylacetone and carbon in phenol ring attached by –OH) in Zr-PF have occurred large drift compared with the chemical shifts of corresponding acetylacetone and hydroxymethyl phenol monomers, indicating that a new chemical bond has been formed through coordination reaction between zirconium atoms in Zr–OH and oxygen atoms in the acetylacetone and hydroxymethyl phenols [16]. The conclusions of NMR confirm to the result of FT-IR.

3.2. Viscosity of zirconium modified phenolic resin (Zr-PF)

A comparison of viscosity–temperature curves of PF and Zr-PF is shown in Fig. 4. The curves show that both PF and Zr-PF have wide temperature range of 30–80 °C and low viscosity of 50–930 mPa s, which is suitable for impregnation; viscosity of the Zr-PF is higher than that of PF from 30 °C to 80 °C. Interestingly, viscosity of both the PF and Zr-PF reduces to the lowest at 80 °C. However, the viscosity of them increases quickly when further increasing the temperature. During the densification cycle in manufacturing carbon/carbon composites, viscosity of the precursor plays an important role in the process of filling the pores and cracks formed during carbonization [17]. As the viscosity of Zr-PF increases, it is more difficult than PF to fill the pores due to the decrease in fluidity, which would decrease the process ability of composites in general.

Table 1
Characteristic absorption peaks of zirconium modified phenolic resin.

The peak of absorption band (cm^{-1})	Chemical bond
3342	–OH stretching of phenolic ring
1597, 1506	C=C stretching of phenolic ring
1477, 1375	Scissoring vibration of $-CH_2-$
1450	Stretching vibration of C=O
1238	Stretching vibration of C–O
1156	Stretching vibration of CH_2-O-CH_2
1024	C–O stretching of hydroxymethyl
888	C–H flexural vibration of phenolic ring meta position
821	C–H flexural vibration of phenolic ring para position
757	C–H flexural vibration of phenolic ring ortho position
560	Vibration of Zr–O

3.3. Thermal stability of zirconium modified phenolic resin (Zr-PF)

TG–DSC was conducted in nitrogen atmosphere to investigate the thermal stability of Zr-PF. Fig. 5 shows the TG–DSC curves of PF and Zr-PF. The weight loss and major reactions during pyrolysis processes are summarized in Table 3. It can be seen that the pyrolysis processes of PF and Zr-PF are similarly, which can be divided into three major reaction regions. In the first region, evolution of water, crosslinked by-products and unreacted oligomers is the main reaction. While compared with PF, there is an extra exothermic peak at 88 °C in the DSC curve of Zr-PF, which corresponds to dehydration of Zr–OH. And this may explain the 6.2% higher weight loss of Zr-PF in the first region. In the second region, there is mainly thermal decomposition and carbonation. The weight loss is about the same for both PF and Zr-PF in this region. However, the peak in the range of 400–450 °C corresponding to the phase formation of ZrO_2 in the DSC curve of Zr-PF is obvious [18]. In the third region, the weight loss of Zr-PF is much lower than that of PF. The reason may be that zirconium atoms were crosslinked with phenolic hydroxyl groups forming new chemical Zr–O bonds, which is 776 kJ mol^{-1}, much higher than C–C bond (345 kJ mol^{-1}). And the stronger chemical bond would hinder the process of pyrolysis and carbonization. Besides the peaks in the range of 1000–1200 °C corresponding to deep carbonation of pyrolytic carbon for both PF and Zr-PF, the peaks at about 994 °C in the DSC curve of Zr-PF are assigned to the phase transformation of m-ZrO_2 to t-ZrO_2 [19].

Although the initial decomposition temperature of PF and Zr-PF is both about 350 °C, the maximum decomposition temperature of Zr-PF is about 700 °C, 100 °C higher than that of PF (about 600 °C). The temperature at the maximum decomposing rate of Zr-PF is 620 °C, an increase of 75 °C compares to that of PF (545 °C). Moreover, the char yield of Zr-PF at 1200 °C is 55%, which is also 8% higher than the latter (47%). Therefore, it can be deduced that the high temperature resistance of PF is improved owing to the introduction of zirconium element. This can be attributed to the higher bond energy of Zr–O and the hyperbranched structure formed during the curing reaction in Zr-PF [20,21].

3.4. Microstructure of carbonized zirconium modified phenolic resin (Zr-PF)

The Raman spectrum of carbonaceous material shows mainly two bands, 1360 cm^{-1} called D peak which corresponds to the defect-induced Raman band, and 1600 cm^{-1} called G peak which corresponds to the "in-plane" displacement of the carbons, indicating the graphite crystal structure [22]. The intensity ratios such as ID/IG and ID/(ID + IG) are proportional to the degree of graphitization, indicating the disorder in carbon materials. The microcrystalline planar size (La) can be calculated as follows [23]:

$$La = 4.35IG/ID$$

The Raman spectra of the carbonized products of the PF and Zr-PF are shown in Fig. 6. And data analysis is listed in Table 4. Compared with PF, the ID/IG value of the carbonized products of Zr-PF decreases from 1.330 to 0.571. It can be noted that the crystal size

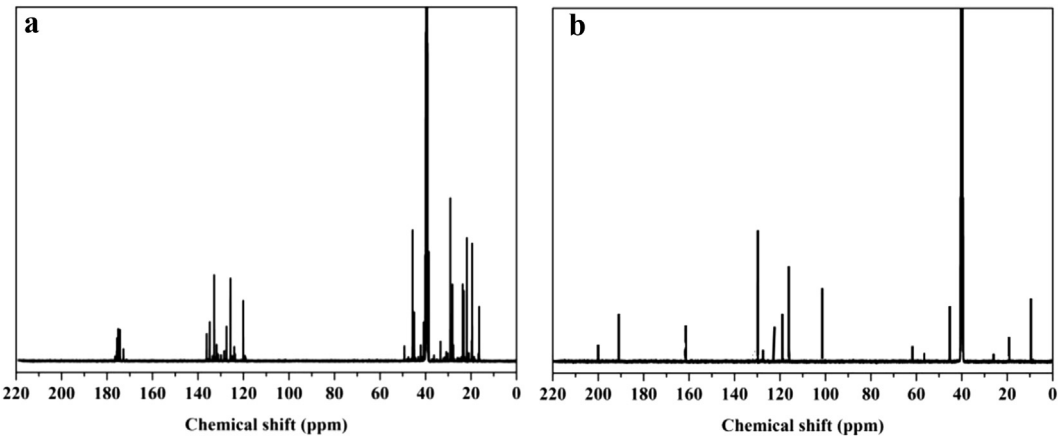

Fig. 3. ^{13}C NMR spectra of ordinary phenolic resin and zirconium modified phenolic resin, a) ordinary phenolic resin, b) zirconium modified phenolic resin.

La of the carbonized products of Zr-PF is 7.61 nm, much larger than that of PF (3.26 nm). The ID/(ID + IG) value of Zr-PF is 0.364, while the value for PF is greater than 50%. These changes demonstrate that the incorporation of zirconium leads to an obvious increase of graphite structure of PF. Zirconium may be incorporated into the graphene cyclic systems, increasing the amount of active sites and reducing the surfacing activation energy of graphitization. Therefore, it can be considered as catalysts for promoting structural order. The reason may be that the metal exhibits a weaker binding to the plane of graphite than it does to the surface of amorphous carbon. Thus, the difference in the adhesive forces between graphite to metal and the amorphous carbon to metal results in the improvement of transformation from amorphous carbon to graphite [24].

The XRD pattern of carbonized Zr-PF at 2000 °C is shown in Fig. 7. The products formed at 2000 °C exhibit sharp peaks in Fig. 7, which would be due to ZrC with high crystallinity. Carbon peaks at 26.8° and 42.8° indicate that carbonized products of Zr-PF are pure ZrC and C during the carbonization. The XRD pattern of carbonized PF at 2000 °C is shown in Fig. 8. Broad peaks, indicating turbostratic carbon structure, are observed at 2θ angles of about 26.6°, 43.5°, 54.8° and 77.7°, respectively. Table 5 lists crystal parameters of the

Table 2
The major chemical shifts of the PF and Zr-PF in the ^{13}C NMR spectra.

Material	Chemical shift/ppm	Description
PF	170–180	Carbon in C=O
PF	120–136	Aromatic carbons
PF	35–50	Methylene bridge carbons
PF	40	Carbon in DMSO solvent
PF	18–30	Methylene
Zr-PF	190–203	C=O in acetylacetone
Zr-PF	161	Carbon in phenol ring attached by –OH
Zr-PF	115–130	Carbon in phenol ring
Zr-PF	62	$-CH_2-$ attached by –OH and phenol ring
Zr-PF	101, 56	$-CH_2-$ in acetylacetone
Zr-PF	40	Carbon in DMSO solvent
Zr-PF	10–30, 42	$-CH_3$ in acetylacetone

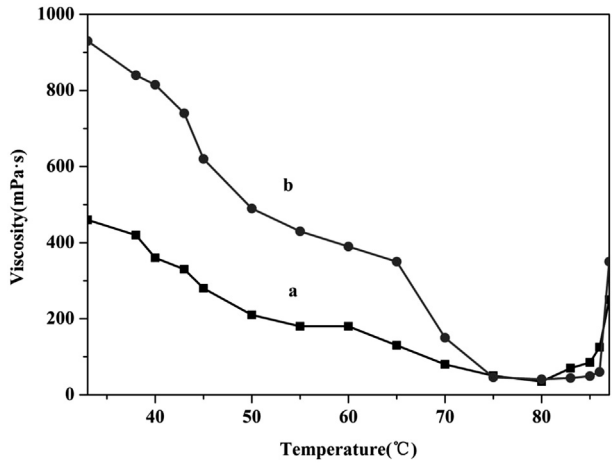

Fig. 4. Viscosity–temperature curves of ordinary phenolic resin and zirconium modified phenolic resin, a) ordinary phenolic resin, b) zirconium modified phenolic resin.

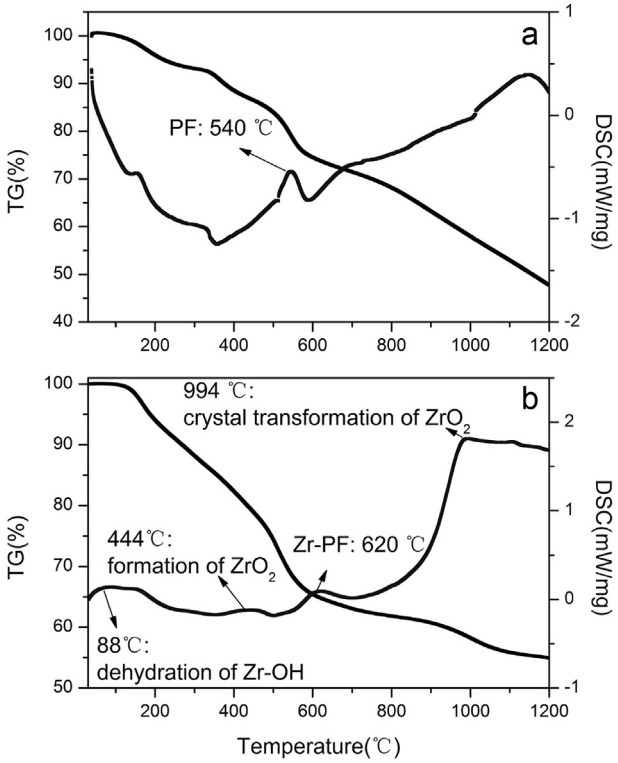

Fig. 5. TG–DSC curves of ordinary phenolic resin and zirconium modified phenolic resin, a) ordinary phenolic resin, b) zirconium modified phenolic resin.

Table 3
The weight loss and major reactions during pyrolysis processes of PF and Zr-PF.

Temperature range/°C	Weight loss/%		Main reactions	
	PF	Zr-PF	PF	Zr-PF
30–350	8.4	14.6	Drying, polycondensation and dehydration between small molecules, curing	Drying, dehydration of Zr–OH, polycondensation and dehydration between small molecules, curing
350–700	20.2	22.4	Pyrolysis and carbonization	Pyrolysis, carbonization and formation of ZrO_2
700–1200	23.8	8.0	Carbonization and structure of matrix carbon becomes ordered	Carbonization, crystal transformation of ZrO_2, structure of matrix carbon becomes ordered
Weight residue at 1200 °C (%)	47	55	—	—

carbonized products of PF and Zr-PF. Compared with PF, the crystallinity of the carbonized products of Zr-PF is greatly improved, showing that a well defined structure is obtained. It is deduced that the presence of zirconium has little effect on the parameters of diffraction peak, but has obvious effect on the parameters of crystallite sizes. The basal spacing d_{002}, crystallite size (La) and crystal thickness (Lc) were calculated by the following expressions [25], respectively:

$$d_{002} = \lambda/(2\sin\theta);$$

$$\mathrm{La} = k_1\lambda/B(10)\cos\theta;$$

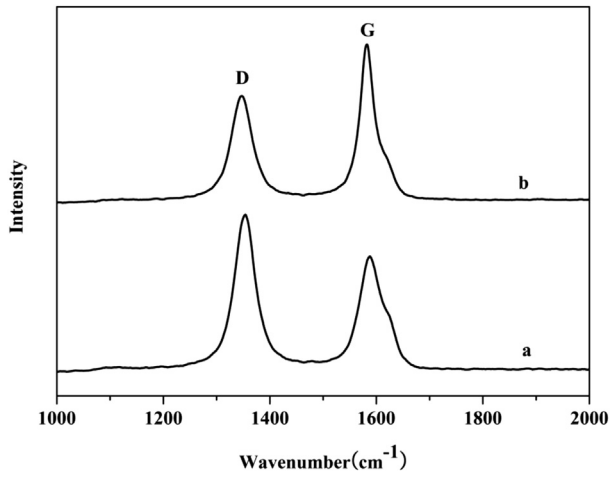

Fig. 6. Raman spectra of carbonized products of ordinary phenolic resin and zirconium modified phenolic resin, a) ordinary phenolic resin, b) zirconium modified phenolic resin.

Table 4
Raman spectra parameters for carbonized PF and Zr-PF.

Sample	ID/IG	ID/(ID + IG)	La (nm)
PF	1.330	0.571	3.26
Zr-PF	0.571	0.364	7.61

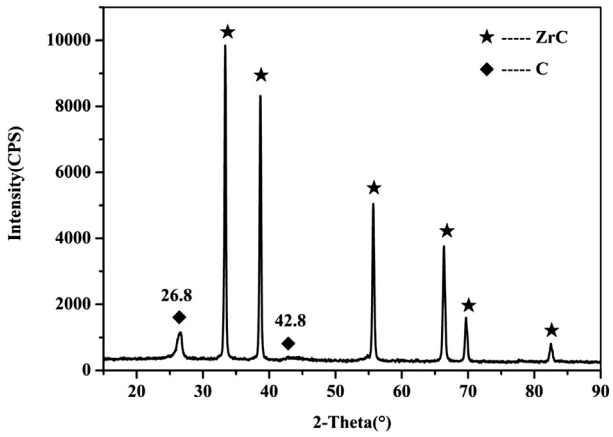

Fig. 7. XRD pattern of carbonized Zr-PF at 2000 °C heat treatment for 2 h in nitrogen.

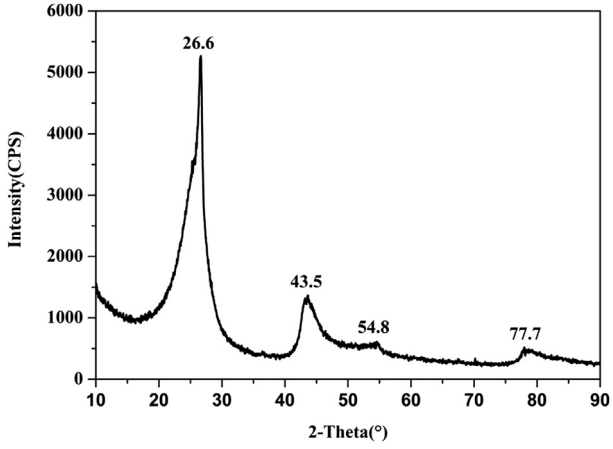

Fig. 8. XRD pattern of carbonized PF at 2000 °C heat treatment for 2 h in nitrogen.

$$\mathrm{Lc} = k_2\lambda/\mathrm{B}(002)\cos\theta;$$

where $\lambda = 0.1541$ nm, apparatus constants k_1 and k_2 are 1.84 and 0.94, respectively, B is the half value width in radians of the X-ray diffraction intensity.

It can be seen that the d_{002} values of the two samples are both lower than 0.3500 nm and the value of carbonized Zr-PF is a little lower than that of carbonized PF, indicating that zirconium may have intercalated into the interlayers of graphite sheets as well as the pores of its networks and leads to the deformation of carbon lattice. Moreover, the La and Lc values of carbonized Zr-PF are both much higher than that of PF. This indicates that the incorporation of zirconium contributes to the growth of crystallite, increasing crystallite height and decreasing interlayer spacing. It is consistent with the result of Raman.

3.5. Morphologies of carbonized zirconium modified phenolic resin (Zr-PF)

The morphologies of the carbonized PF and Zr-PF are shown in Fig. 9. According to the SEM images, there are many pores with

Table 5
Parameters of (002) and (10) diffraction peaks for carbonized PF and Zr-PF.

Sample	2θ (002)	2θ (100)	d_{002}/nm	La/nm	Lc/nm
PF	26.6	43.5	0.3470	29.90	23.89
Zr-PF	26.8	42.8	0.3329	44.79	29.21

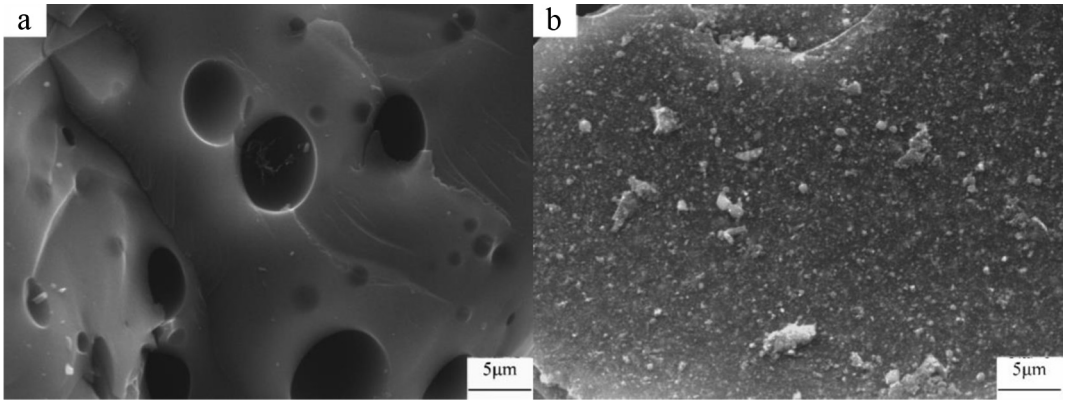

Fig. 9. SEM images of carbonized PF and Zr-PF at 2000 °C heat treatment for 2 h in nitrogen, a) carbonized PF, b) carbonized Zr-PF.

different sizes distributed uniformly in carbon matrix of PF. These pores are caused by the escape of gas molecules. On the contrary, the carbonized products of Zr-PF are dense and uniform without obvious pore defects, suggesting that using Zr-PF as a precursor for impregnation may shorten the time of filling the pores and cracks formed during carbonization and improve impregnation efficiency. Moreover, the ZrC particles smaller than 200 nm are uniformly dispersed throughout the carbon matrix, which indicates that zirconium exhibits good miscibility in organic phases [26]. On the other hand, precipitation of the ceramic particles was accompanied by the pyrolysis of the polymer and bonds cleavage, which avoids the rapid crystallization and crystal growth.

4. Conclusions

A kind of zirconium modified phenolic resin (Zr-PF) was synthesized by using phenol, paraformaldehyde, $ZrOCl_2 \cdot 8H_2O$, acetylacetone, ethanol, H_2O_2 as raw materials and zirconium was successfully incorporated into the reaction product. Viscosity of the Zr-PF is 50–930 mPa s during the temperature range of 30–80 °C and it is suitable for impregnation. Thermal stability of the Zr-PF is obviously improved and the char yield of it at 1200 °C is 55%, 8% higher than that of PF. What is more, zirconium incorporation can also affect the microstructure and greatly improve the degree of graphitization of the carbonized products. The ID/(ID + IG) value of carbonized Zr-PF decreases from 0.571 (carbonized PF) to 0.364. And the crystallite size of carbonized Zr-PF increases from 29.90 nm (carbonized PF) to 44.79 nm. The crystallite height is increased and the interlayer spacing is decreased because of the incorporation of zirconium. In addition, the morphology of the carbonized Zr-PF changes from poor structure with many pore defects into dense and uniform matrix with uniformly dispersed ZrC particles.

Acknowledgments

This work has been supported by the National Natural Science Foundation of China under Grant No. 51272213, 51221001 and 51202093, and supported by the "111" Project under Grant No. B08040 and the Research Fund of the State Key Laboratory of Solidification Processing (NWPU), China (Grant No. 73-QP-2010).

References

[1] Bindu RL, Reghunadhan Nair CP, Ninan KN. Phenolic resins with phenyl maleimide functions: thermal characteristics and laminate composite properties. J Appl Polym Sci 2001;80:1664–74.
[2] Song YZ, Qiu HP, Zhai GT, Shi JL, Song JR, Liu L. Study on densification for carbon/ceramic composites with thermosetting phenolic resins. Carbon Tech 2001;5:17–9.
[3] Krıstkova M, Filip P, Weiss Z, Peter R. Influence of metals on the phenol–formaldehyde resin degradation in friction composites. Polym Degrad Stab 2004;84:49–60.
[4] Abdalla MO, Ludwick A, Mitchell T. Boron-modified phenolic resins for high performance applications. Polymer 2003;44:7353–9.
[5] Gao JG, Xia LY, Liu YF. Structure of a boron-containing bisphenol-F formaldehyde resin and kinetics of its thermal degradation. Polym Degrad Stab 2004;83:71–7.
[6] Li XT, Shi JL, Zhang GB, Zhang H, Guo QG, Liu L. Effect of ZrB_2 on the ablation properties of carbon composites. Mater Lett 2006;60:892–6.
[7] Jayaseelan DD, Sá RG, Brown P, Le WE. Reactive in filtration processing (RIP) of ultra high temperature ceramics (UHTC) into porous C/C composite tubes. J Eur Ceram Soc 2011;31:361–8.
[8] Fu QG, Li HJ, Shen XT, Li KZ. Domestic research process of matrix modification for carbon/carbon composites. Mater China 2011;11:6–12.
[9] Marcalo J, Gibson JK. Gas-phase energetics of actinide oxides: an assessment of neutral and cationic monoxides and dioxides from thorium to curium. J Phys Chem A 2009;113(45):12599–606.
[10] Xu SH, Zhang FY, Kang Q, Liu SH, Cai QY. The effect of magnetic field on the catalytic graphitization of phenolic resin in the presence of Fe-Ni. Carbon 2009;47:3233–7.
[11] Wang YG, Shi TJ, Li Z. Preparation and characterization of zirconium modified phenolic resin. Chem Pro Polym Mater 2009;7(4):37–9.
[12] Liu HY, Liu GS, Pei SG, Chen Y, Liu JQ. Preparation of zirconia fibers cotton by centrifugal spinning of polyacetylacetonatozirconium spinning solution. Bull Chin Ceram Soc 2011;6:1410–4.
[13] Tao XY, Qiu WF, Li H, Zhao T, Wei XY. New route to synthesize preceramic polymers for zirconium carbide. Chin Chem Lett 2012;9:1075–8.
[14] Benard F, Campistron I, Laguerre A, Laval F. Influence of silica fillers during the electron irradiations of DGEBA/TETA epoxy resins, part I: study of the chemical modification on model compounds. Polym Degrad Stab 2006;91:2110–8.
[15] Huang AYC, Wang FY, Ma CCM, Wu HD. Thermodynamic properties affect the molecular motion of novolac type phenolic resin blend with polyamide. Eur Polym J 2003;39:225–31.
[16] Zhao JK, Han XW, Liu XM, Bao XH, Hang JF, Jiang B. The mechanism of asymmetric reduction catalyzed by a C_2 symmetric bis-amino alcohol catalyst. Sci Chin Ser B 2000;43(1):40–50.
[17] Bansal D, Pillay S, Vaidya U. Processing and characterization of nanographene platelets modified phenolic resin as a precursor to carbon/carbon composites – part I. J Reinf Plast Compos 2013;32(9):585–92.
[18] Dodd AC, McCormick PG. Synthesis of nanocrystalline ZrO_2 powders by mechanochemical reaction of $ZrCl_4$ with LiOH. J Eur Ceram Soc 2002;22:1823–9.
[19] Noda LK, Goncalves NS, Borba SM, Silveira JA. Raman spectroscopy and thermal analysis of sulfated ZrO_2 prepared by two synthesis routes. Vib Spectrosc 2007;44:101–7.
[20] Liu YH, Jing XL. Pyrolysis and structure of hyperbranched polyborate modified phenolic resins. Carbon 2007;45:1965–71.
[21] Tu JH, Zhang LB, Peng JH, Zhang SM, Pu JZ, Xia HY, et al. Fabrication mechanism and structure of glass-like carbons derived from phenolic resin. Carbon Tech 2005;24:21–9.
[22] Zhou DF, Zhao YL, Hao J, Ma Y, Zhang XY, Su ZM, et al. Effect of $ZnCl_2$ doping on the structure and properties of carbonized phenolic resin material. Chem J Chin Univ 2013;12:2296–9.
[23] Zhang Y, Shen SH, Liu YJ. The effect of titanium incorporation on the thermal stability of phenol-formaldehyde resin and its carbonization microstructure. Polym Degrad Stab 2013;98:514–8.
[24] Anton R. On the reaction kinetics of Ni with amorphous carbon. Carbon 2008;46:656–62.
[25] Liu CL, Dong WS, Song JR, Liu L. Evolution of microstructure and properties of phenolic fibers during carbonization. Mater Sci Eng A 2007;459:347–54.
[26] Chiang CL, Ma CC. Synthesis, characterization, thermal properties and flame retardance of novel phenolic resin/silica nanocomposites. Polym Degrad Stab 2004;83:207–14.